MONITORING CORE MEASUREMENTS WITH HIGH-RESOLUTION TEMPERATURE ARRAYS

James J. Howard and Keith C. Hester
University of Tulsa, Eni S.p.A.

This paper was prepared for presentation at the International Symposium of the Society of Core Analysts held in Trondheim, Norway, 27-30 August 2018

ABSTRACT

While Distributed Temperature Sensing (DTS) has become a commonly used tool in reservoir studies, the technology has not seen widespread use in SCAL projects. Most core-scale experiments attempt to control temperature at a constant value rather than monitor temperature changes within a sample during a test. High-resolution temperature arrays are available that measure changes in temperature of 0.1^{o}C at 1 mm resolution. The Optical Backscatter Reflectance (OBR) fiber senses both temperature and strain that can be separated through experiment design and signal processing. These OBR fibers are sensitive enough to monitor temperature changes associated with endo- and exothermic chemical reactions associated with mineral dissolution/precipitation, or fluid front movements in steam-assisted gravity drainage of heavy oil tests. An example of the use of a distributed temperature array is in the monitoring of natural gas hydrate formation and dissociation in a sand pack as CO2 is exchanged with the naturally occurring CH4 in the hydrate structure. A fiber optic array was placed within a narrow diameter PEEK tube as the sand pack was constructed. The PEEK tube held the fiber optic in place so that the sensed signal was temperature only and did not include any strain effects. The OBR was set up to acquire a temperature array every 30 seconds during the test at 5 mm spacings. The core holder was placed in a MRI that provided additional spatial information on hydrate formation during the test that was compared with the OBR results. Initial hydrate formation resulted in a several degrees increase in temperature at the inlet end of the cell that with time progressed down the length of the cell. The temperature array and MRI images both showed the non-uniform nature of hydrate formation and subsequent dissociation of the hydrate when N2 was injected into the cell as a permeability enhancement step. The faster response of the OBR array compared to the time required to acquire MRI images provided additional detail in the sequence of hydrate formation and dissociation during CH4-CO2 exchange. The limitation to the OBR array was that it only sensed temperature fluctuations proximal to the fiber as a function of the hydrate system's thermal conductivity.

INTRODUCTION

Measurable temperature changes are associated with a number of geochemical reactions in porous media that occur with phase changes connected with mineral precipitation and

dissolution. While thermodynamic data may indicate large temperature changes with an idealized geochemical reaction, the actual measured temperatures are often much smaller because of volume and heat flow constraints. Most experiments monitor a single averaged temperature of the reaction vessel and miss out on details of the geochemical processes that occur in heterogeneous porous media. Multiple temperature probes are one way to capture some of this detail.

Natural gas hydrates are characterized by well-defined heats of formation that translate to measurable temperature changes observed during formation and dissociation. [1,2] Most of the observations on temperature change were collected on simple water-gas-hydrate systems measured in bulk. This study reports measurements of temperature changes as hydrates formed and dissociated in a porous medium.

A series of laboratory experiments designed to support the field trial of CO_2-CH_4 exchange mechanisms investigated the role of injection gas composition on the effectiveness of the injection process and the actual exchange. The success of the Ignik Sikumi #1 field trial in 2011-12 was in part due to these laboratory tests. [4] These experiments followed the design of earlier studies that formed methane hydrate in porous media, introduced CO_2 into the system while using MRI methods to monitor the progress of the formation and dissociation. [3,5] The laboratory experiments became more elaborate as the interest shifted from simple formation and dissociation rates to questions involving the permeability of the porous media and the stability of the hydrate-bearing sediment. [6,7,8] These experiments included a series of sensors attached to the sample holder, (e.g. electrodes, ultrasonic transducers) that measured electrical conductivity and sonic velocities along with the standard monitoring of pressure temperature and fluid volumes for the duration of the test. The MRI images collected during many of these early experiments illustrated non-uniform hydrate formation and dissociation throughout the porous media. Only in rare cases under special conditions was hydrate formation observed to follow a simple front-like displacement down the length of the core. For several of these new experiments an additional temperature sensor was added to the design beyond the thermocouples attached to the sample holder. A fiber optic array was placed within the porous media and used to monitor small changes in temperature at distinct points along the length of the sample during hydrate formation and exchange processes.

EXPERIMENTAL DESIGN AND SAMPLES

The basic design was centered around a MRI-compatible core holder that had sufficient inlet and outlet ports on the end-plugs to connect to a series of pumps that controlled the introduction of various fluids to the sample. These pumps monitored the volumes of injected fluids, including water, methane and CO_2, and their pressures. A separate dedicated pump controlled the confining pressure on the sample. The temperature of the sample was managed by controlling the temperature of the NMR-insensitive liquid (Fluorinert, 3M) that flowed in the space between the core holder and the sample's confinement sleeve that also handled the confining pressure. A temperature probe was

located in this open space between sleeve and core holder that monitored the overall temperature of the system.

A sand pack was used for these experiments rather than the pieces of sandstone core that were the focus of the first tests of the CO_2-CH_4 exchange mechanism. A mold using Teflon shrink wrap tubing was placed on top of one of the core holder's end pieces and filled with ~100 grams of Ottawa F110 sand. This sand has an average grain size of 100 microns and is used in a number of hydrates experiments. [9] A small diameter, 1 mm, PEEK tube was positioned in the center of the mold with one end inserted through one of the ports in the end piece. The sand was added in small amounts with intervals of shaking the mold to encourage closest packing of the sand grains, especially around the PEEK tube. Once the mold was filled with sand and a volume of water added to the sand, the top end piece of the core holder was secured to the shrink-wrap mold. Once the core holder was assembled and the various fluid lines connected to their pumps, the fiber optic line was threaded through the dedicated inlet port, through the PEEK tube in the sand pack and then out through its dedicated line in the outlet end piece (Figure 1).

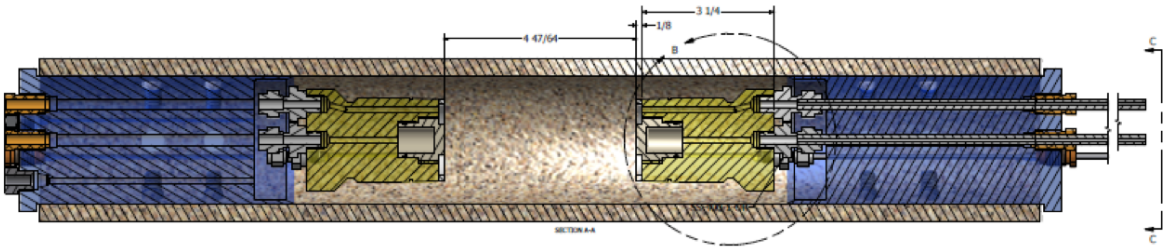

Figure 1. Core holder with four ports on each end that allows for multiple sensors to be included in the experimental design. Sand pack is located at the center of the holder.

As with earlier experiments, MRI images were collected throughout the test as a way to monitor changes in fluid and hydrate saturations. The MRI (2.0T Varian) was sensitive to hydrogen nuclei in a liquid or dense gas state (e.g. water, methane at 8.4 MPa), but the limitations of that instrument's probe made it insensitive to hydrogen nuclei in the solid state (ice, hydrate).

A distributed temperature sensor probe was used to monitor temperature changes along the length of the sand pack during the hydrate formation and exchange processes. The Optical Backscatter Reflectance (OBR) fiber optic cable is sensitive to changes in both temperature and stress, the latter that might occur if the cable moved in the sample during the test. One consequence of using the PEEK tube to thread the fiber through the sample was that once the core holder was positioned in the MRI it did not move for the duration of the test. Data acquisition parameters were defined to collect stations every 0.5 cm at a time interval of 30 seconds during the entire experiment. The data acquisition was restarted at major transition points in the experiment as a data management precaution, but had the downside that sometimes the internal calibration was altered. Absolute

temperature values therefore are sometimes in error, though the relative changes in temperature are internally correct. The sensor has a sensitivity of 0.1°C.

RESULTS

The assembled sand packs had a length of roughly 11 cm and a diameter of 5.05 cm, creating a bulk volume of 225 cm^3. The pore volumes ranged from 90 to 100 cm^3, resulting in a porosity of approximately 40%. The initial water saturation created by adding water during the construction stage ranged from 58 to 75%. Initial permeability of the water saturated sand pack prior to cooling was 200 to 400 mD. The formation of hydrate dropped that permeability down to 30 mD. Permeability of the system remained above 10 mD even after the addition of more water to the remaining gas-filled pores and the introduction of CO_2 that formed even more hydrate.

The test included a period of methane hydrate formation after the cell was cooled to 4°C (Figure 2). MRI signal intensity averaged over the entire sample was used to monitor the progress of the experiment. Most of the water was converted to hydrate and the initial hydrate saturation was 72%. The effective porosity was 11% and the permeability was 30 mD. After the hydrate formation slowed down a short stage of water injection increased the total MRI signal. This additional water filled most of the air-filled pores with liquid and created a situation that more closely simulated an actual hydrate reservoir. The N_2 injection stage was intended to dissociate some of the hydrate and increase the overall permeability of the sand pack. The increase in MRI signal resulted from the loss of about half of the initial hydrate. The final stage was the introduction of a CO_2-N_2 gas mixture that resulted in the formation of a CO_2 hydrate and the production of some methane. Separate analyses of the produced gas composition verified the exchange. [4]

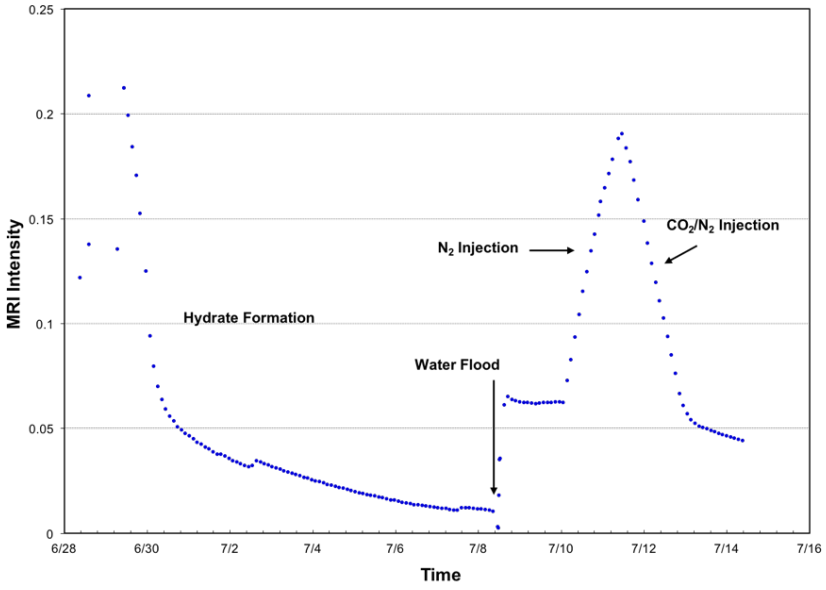

Figure 2. Overview of experiment that started with initial hydrate formation through the final step of injecting a CO_2/N_2 gas. MRI intensity indicates the amount of free water in the sample that has not converted to hydrate.

The sand pack had an initial water saturation of approximately 60%, with the remaining pore volume filled with air. As methane was injected at the inlet end and the temperature of the cell cooled from room temperature to 4°C hydrate began to form. Temperature curves from the front and back platen in the core holder along with a temperature collected at the center of the sand pack provided several insights into the hydrate nucleation process (Figure 3). The volume of methane consumed as it first dissolved in the cold water then followed by actual hydrate formation was captured by the pump connected to the sample holder. The small heat of methane solution at four hours was observed in the temperature sensor located in the core, but not at the platen ends. The second event of methane consumption represented the formation of hydrate that was captured with a several degree increase in temperature monitored in the core and at the end pieces. A third temperature spike at fourteen hours corresponded to a decrease in the methane consumption rate as hydrate formation reached an end.

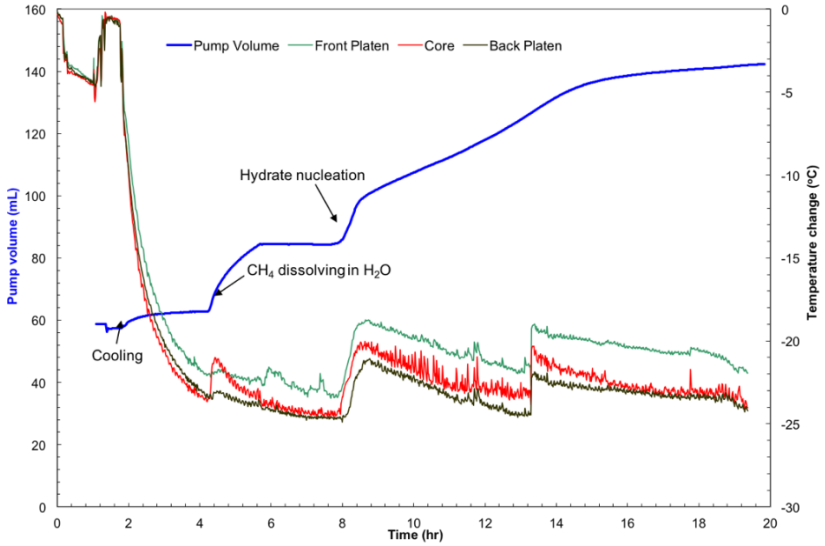

Figure 3. Methane consumption (blue curve) along with temperature sensors in the core and at the end pieces define several stages in hydrate formation.

The combination of MRI images and the profile temperature curves provided more insights into the hydrate formation process than could be discerned from the gas consumption curve (Figure 4). The MRI image at the earliest stage of the hydrate formation (top image) is dominated by "warm" colors that indicate the presence of sensible hydrogen (i.e. water). As hydrate formed during the cooling the MRI responded to a reduced signal intensity as water was converted to hydrate as illustrated with "cooler" colors on the images (2nd through 4th images). The initial image has a small spot in the lower portion of the sample, approximately one-third the distance from the inlet

(left side) that suggests the region where hydrate formation started. The subsequent images show that hydrate formation was localized on the bottom of the sand pack and slowly moved upwards during the several days of initial hydrate formation. The temperature profiles of the sand pack were averaged over the time required to collect the MRI images, approximately 2 hours. The profile for the initial image (1a-13r) was uniform along the length of the sand pack with a slight hint of temperature increase at slice 13. The subsequent temperature profiles had significant temperature increases at the inlet end of the cell, increasing from 1.4°C to 2.4°C as more hydrate was formed.

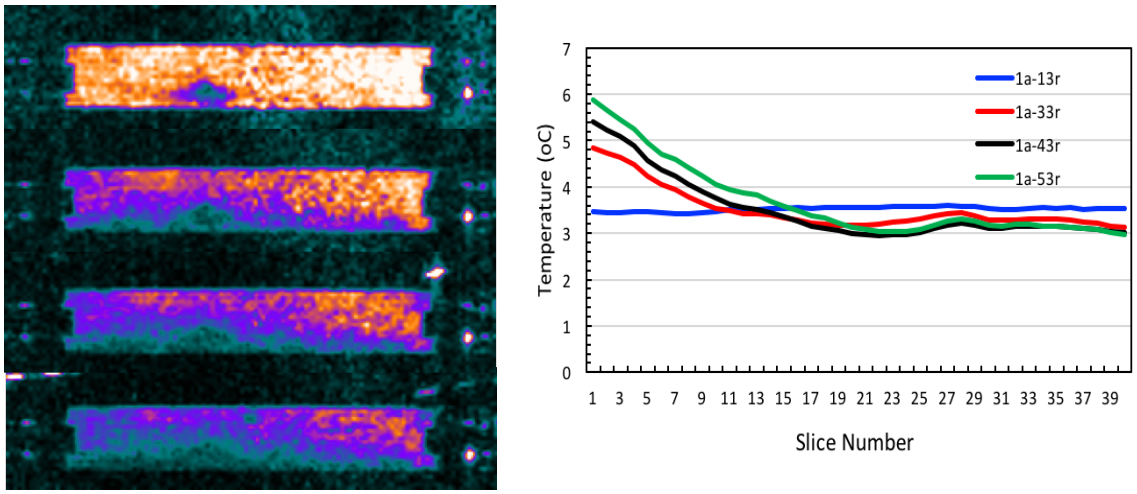

Figure 4. MRI images of sand pack during initial hydrate formation collected over a two-day period (top to bottom) along with temperature profiles collected at the same time. Hydrate formed initially at bottom of image on left side (inlet) as represented by blue (cooler colors).

Injection of N_2 was included in the experiment to remove hydrate from some of the pores, especially at the inlet end of the core. This resulted in the dissociation of some of the hydrate, accompanied by a drop in temperature and the release of some of the methane from the hydrate (Figure 5). The starting point of this stage was defined by the temperature profile 1c-01 and the top most MRI image. The N2 injection increased the sample permeability from the 30 mD created by the initial hydrate formation to 55 mD. The dissociation of hydrate during N_2 injection over the next 64 hours was illustrated by the drop in temperature profiles (1c-25 and 1d-01) and the return of free water signal in the MRI images (2^{nd} and 3^{rd} images). The images suggested more hydrate dissociation closer to the inlet end of the sand pack, while the temperature profiles showed a smaller drop in temperature compared to the starting point. These 2D slices of the entire 3D sand pack volume were selected as the centermost (16 of 32) and often did not represent the total distribution of hydrate and free water phases in the sample.

The N_2 injection step was followed by the injection of a N_2-CO_2 gas mixture over the following 36 hours. The CO_2 formed new hydrate and exchanged with methane in hydrate structure, releasing additional methane. The hydrate formation resulted in increased temperatures along the length of the core, with the larger change taking place

closer to the inlet end (profiles 1d-07 and 1d-15). MRI images collected during the N_2-CO_2 injection showed the changes in hydrate saturation and the preferential dissociation near the inlet end during the N_2 injection as the total hydrate saturation increased. The final hydrate saturation was approximately 80% and the measured permeability was 10 mD after the completion of the N_2-CO_2 injection. Methane was collected at the outlet end and the mechanism of CH_4-CO_2 exchange was verified. [4]

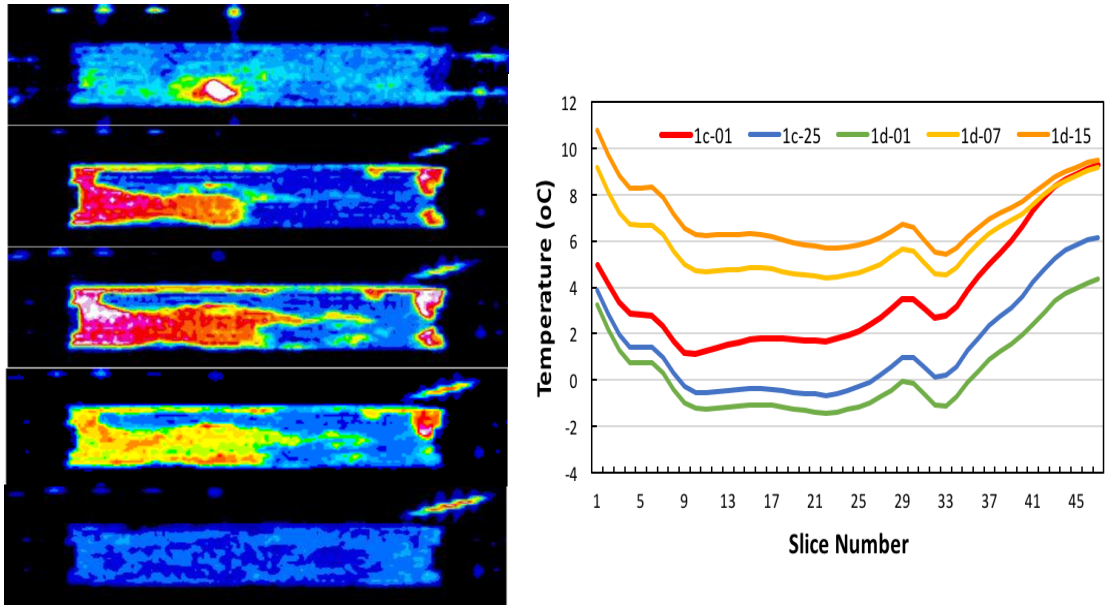

Figure 5. Temperature profiles and MRI images collected at start of N_2 injection (1c-01, top image) and the dissociation that accompanied the injection (1c-25, 1d-01, 2nd and 3rd images). This was followed by N_2-CO_2 injection that reformed hydrate (1d-07, 4th image) to an end point (1d-15, bottom image).

A second experiment investigated the thermal effects associated with depressurization below the hydrate stability (Figure 6). Pressure was dropped suddenly from the initial 1200 psi to 600 psi and then an additional 400 psi down to 200 psi over an 18-hour period. The MRI intensity measurements were collected at an interval of 13 minutes. There was a large drop in temperature associated with the drop in large initial drop in pressure that was attributed to gas expansion. As the pressure was slowly dropped from 600 psi the temperature continued to drop at a much slower rate. There was a lag of roughly four hours before there was sufficient MRI signal to show the dissociation of the hydrate into its constituent water and methane phases. The temperature stabilized halfway through the pressure decline and while the averaged MRI intensity was still growing. MRI profiles were acquired with very fast scans for this test compared to the 2.5-hour scans used in the initial test so the signal quality was not as good, but sufficient to observe general trends.

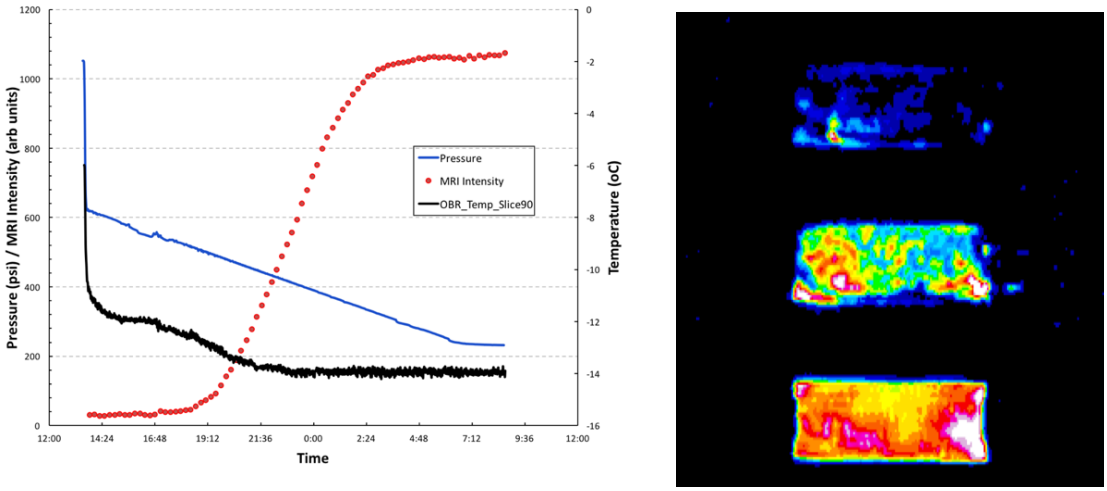

Figure 6. One-day depressurization experiment that followed temperature and MRI intensity trends after pressure was dropped below stability pressure and then slowly ramped downward. MRI 2D slices of Depressurization experiment collected at the beginning of dissociation (top), when the temperature stabilized (middle) and at the end of the depressurization period (bottom).

DISCUSSION

The increase in temperature of several degrees centigrade that was observed during hydrate formation was in agreement with an earlier study the monitored hydrate formation in a reactor vessel filled with sediment. [10] That experiment placed several thermocouples at various depths in the sediment mixture and monitored temperature during cooling and hydrate formation. That experiment also observed very rapid temperature transients during the hydrate formation that matched the temperature events recorded in this study (Figure 3).

The combination of imaging and temperature measurements for monitoring hydrate growth and exchange reactions is complementary, each provides a distinct view of the process and the mechanisms. MRI imaging is ideal because it can easily distinguish between free water and hydrate, though it is limited in that it cannot resolve exchange reactions that occur in the hydrate state. Previous work showed that within the time frame of an MRI image, 15 to 180 minutes, the uniformity of the image during exchange of CO_2 for CH_4 indicated that large-scale dissociation was not the mechanism of exchange. This was not to imply a solid-state reaction since the reaction rates were far too fast for that process. Instead, localized and rapid dissociation and reformation that took place at times much faster than MRI time resolution allowed.

Temperature measurements also are sensitive to changes in state of the water – hydrate system, though perhaps not as robust as MRI imaging. The time constant for temperature measurements is much faster, essentially instantaneous. The introduction of a fiber-optic line into the reactor cell or sediment volume allows for high spatial resolution, fast-time

acquisition temperature data. The small perturbations in the temperature array eventually can be matched with even higher resolution MRI imaging.

The images collected for this study were limited by capabilities of the older generation instrument and the demands of trying to capture water signals with their long T_1 recovery times. A test that followed these temperature experiments showed how adjustments to the image acquisition parameters could improve the resolution of the images (Figure 7). The key adjustment was to dope the water used in the test with $CuSO_4$, which dramatically decreased the T_1 relaxation time constant of the water from 1.3 seconds to 50 milliseconds. This allowed for a significant reduction in recovery time for the measurement, meaning more scans per unit of time. The second adjustment was to increase the applied magnetic field gradient, which resulted in more voxels per unit volume. In this study the original scan created a transverse slice of 32 x 32 voxels. As the resolution was improved to 64 x 64 and ultimately 128 x 128 greater detail was seen in the images. The pore space filled with free water was represented by "brighter" colors while the hydrate-filled pores were darker. The improved resolution highlighted the non-uniform nature of the actual hydrate distribution in these sand packs.

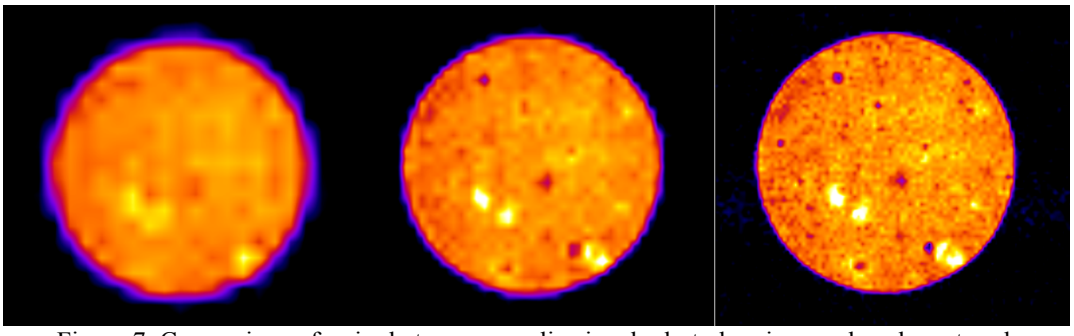

Figure 7. Comparison of a single transverse slice in a hydrate-bearing sand pack captured at 32 x 32 resolution (left), 64 x 64 (center) and 128 x 128 (right). Increased signal intensity denoted by brighter colors represents free water. Hydrate-bearing regions are darker.

The temperature profile along the length of the sand pack has the potential to provide insights into the kinetics of hydrate formation in a porous medium, especially if the sand pack can be monitored throughout by imaging technologies to detect the presence of hydrate or its loss due to dissociation. High-resolution micro-CT or MRI methods are available to generate snap shots of the sample's pore and grain volumes. The limitation lies in the positioning of the fiber optic within the sand pack. While it provides detailed information along the length of the sample, its radial resolution is quite limited. The temperature profile is essentially a 1D measurement in a 3D volume. Improvements in imaging technology should allow for improved comparison of the temperature and hydrate monitoring measurements.

CONCLUSION

A high-resolution optical fiber used to monitor temperature fluctuations associated with geochemical reactions in porous media can be added to the experimentalists' toolbox. This approach generates spatially resolved thermal data that can be used in turn to evaluate heat flow conditions in an experimental setup. The experiment design has to include a means to limit movement of the fiber during the test so that it responds only to temperature fluctuations and not strain. The combined temperature measurements and MRI images showed that hydrate formation and dissociation was non-uniformly distributed along the length of the sample, thus providing new insights not readily obtainable by other experimental techniques. The combination of spatial temperature measurements and sequential imaging opens up new opportunities to measure heat flow and heats of reaction in a wide variety of low-temperature diagenetic scenarios.

ACKNOWLEDGEMENTS

The authors wish to acknowledge Jim Stevens for his laboratory expertise in the design and execution of this study. Funding for the Ignik Sikumi field project was provided by U.S. DOE, JOGMEC and ConocoPhillips.

REFERENCES

[1] E.D. Sloan and C.A. Koh, *Clathrate Hydrates of Natural Gases, 2007*.

[2] Y.F. Makogon, *Hydrates of Hydrocarbons, 1997*.

[3] J. Stevens, B. Baldwin, A. Graue, G. Ersland, J. Husebo, and J. Howard, "Measurements of Hydrate Formation in Sandstones", *Petrophysics,* 2008.

[4] D. Schoderbek, H. Farrell, K. Hester, J. Howard, K. Raterman, S. Silpngarmlert, K. L. Martin, B. Smith, and P. Klein, "ConocoPhillips Gas Hydrate Production Test Final Technical Report", *U.S. Dept. Energy Report DE-NT0006553,* 2013.

[5] B. Baldwin, J. Stevens, J. Howard, A. Graue, B. Kvamme, E. Aspenes G. Ersland, J. Husebo, and D. Zornes, "Using Magnetic Resonance Imaging to Monitor CH4 Hydrate Formation and Spontaneous Conversion of CH_4 Hydrate to CO_2 Hydrate in Porous Media", *Magnetic Resonance Imaging*, 2009.

[6] J. Howard, K. Hester, J. Stevens and M. Rydzy, "Ultrasonic Velocity Measurements During Experimental CH_4 Hydrate Formation and During CO_2 Exchange", *Proceedings of the 7th International Conference on Gas Hydrates,*2011.

[7[K. Hester, J. Howard and J. Stevens, "Composition Studies to Determine Rate and Extent of CO_2 Exchange in a Hydrate-Bearing Core", *Proceedings of the 7th International Conference on Gas Hydrates*, 2011.

[8] S. Almenningen, H. Juliussen, G. Ersland, "Permeability Measurements on Hydrate-Bearing Sandstone Cores with Excess Water", *International Symposium of Society of Core Analysts*, 2016.

[9] W. Waite, J. Santamarina, S. Chong, J. Grozic, K. Hester, J. Howard, et al. "Inter-Laboratory Comparison of Wave Velocity Measurements in a Sand under Hydrate-Bearing and other Set Conditions", *Proceedings of the 7th International Conference on Gas Hydrates*, 2011

[10] B. Liu, W. Pang, B. Peng, C. Sun and G. Chen "Heat Transfer Related to Gas Hydrate Formation/Dissociation, Developments in Heat Transfer", *Developments in Heat Transfer/Heat Transfer Related to Gas-Hydrate Formation Dissociation*, 2011.